Robust and Fully Automated Conformal Mesh Generation for Complex

Stefan Benkler[1], Harald Songoro[2], Nicolas Chavannes[1], Niels Kuster[1]

[1]Foundation for Research on Information Technologies in Society [2]Schmid & Partner Engineering AG, Zurich, Switzerland

INTRODUCTION

The most successfully used technique in electromagnetic (EM) computations is the Finite-Difference Time-Domain method (FDTD, Yee 1966). However, a well known deficiency is that the staircased meshing can lead to inaccuracies in the geometrical discretization of complex models. Conformal meshing and locally (near material interfaces) modified Yee update schemes can be used to overcome this deficiency. However, for the processing of complex simulation settings key issues such as the robustness of the conformal mesher and stability of the modified Yee scheme need to be addressed.

OBJECTIVES

The objectives of this study thus were the development and implementation of novel and robust 3-D CAD analysis algorithms for the fully automated generation of locally conformal FDTD meshes from arbitrarily complex geometries. Furthermore the additional geometric information is incorporated into the FDTD updating algorithm to achieve the same accuracy on a coarser grid, generating substantial savings in simulation time and memory consumption.

METHOD: CAD BASED GENERATION OF CONFORMAL FDTD MESHES

In particular for complex geometries, there is a strong need to automate the material property assignement to each computational cell. In the literature several attemps have been made (e.g., [4]) to use CAD data to extract the cell's material properties. The CAD data consists of a surface triangle description of the scenery to simulate. The result is a (conformal) object description of the scenery on the computational grid.

The addressed and presented problems are the algorithmic complexity and the handling of special cases as well as numerical difficulties with poorly shaped triangles. The difficulties are the same for staircasing and conformal discretization.

Overview of the Discretization

The grid lines are intersected with triangle mesh representing the object's surface. Each grid line thus knows if and where the object is hit. With the scan line conversion algorithm (computer graphics, figure 4) all necessary data (dielectric staircasing voxels, staircasing PxC voxels, conform voxels) can be extracted out of these hit-points (called entry and exit point).

Speed Optimizations

- Calculation of the intersection points: Instead of finding the triangles intersecting a grid line (loop over grid lines, normal approach in computer graphics), all grid lines which intersect a triangle are determined (loop over triangles). Because of the rectilinear grid, the latter approach can be implemented very efficiently.

- Use of scan conversion algorithm ideas (see figure 4): For example, the computationally relatively expensive algorithm to determine conformal cells is only performend on those cells in 'light blue' (see figure 4); no other cells are considered, since conformal cells are not possible in other locations. This idea is used throughout the code:
  - Completing the fourth PxC edge on a face
  - Consistency check: verifying that a point crossed by three perpendicular grid lines is inside the object (or outside) in each direction.
  - etc.

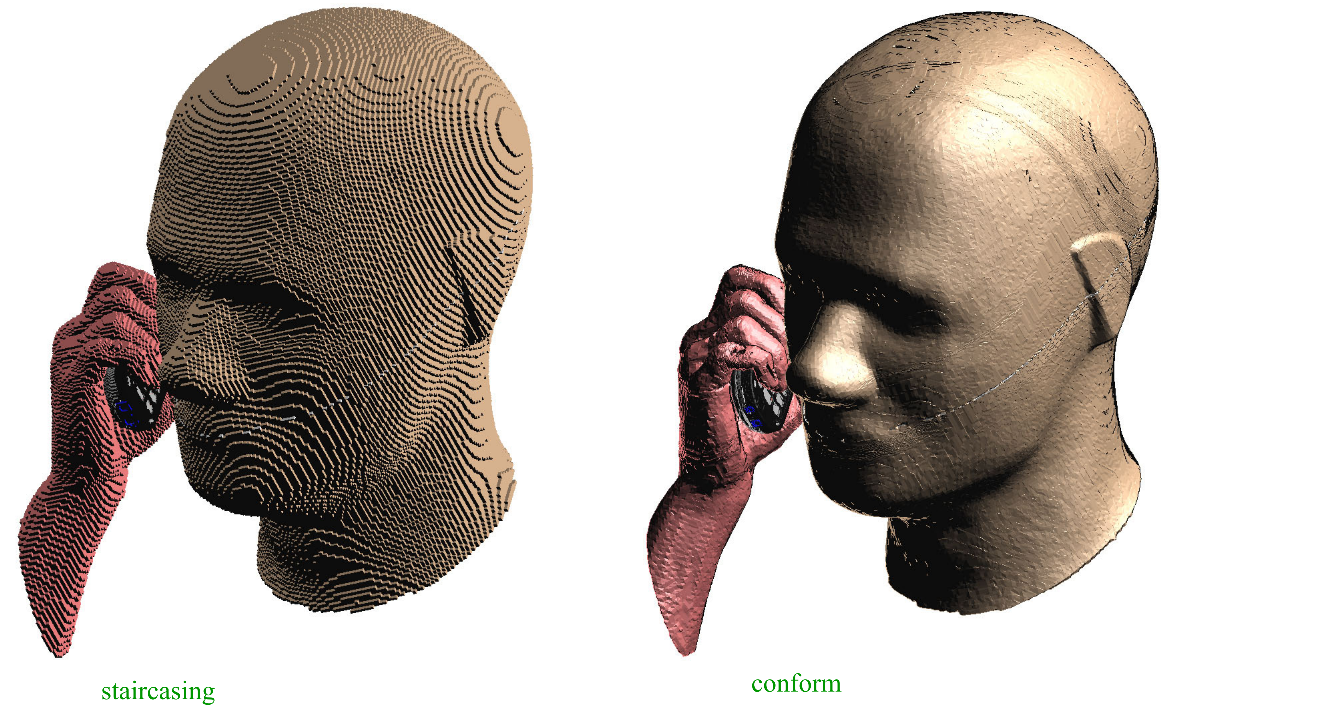

Figure 2: Staircasing and conformal discretization of a SAM head, hand and a mobile phone with a grid of 127x92x133.

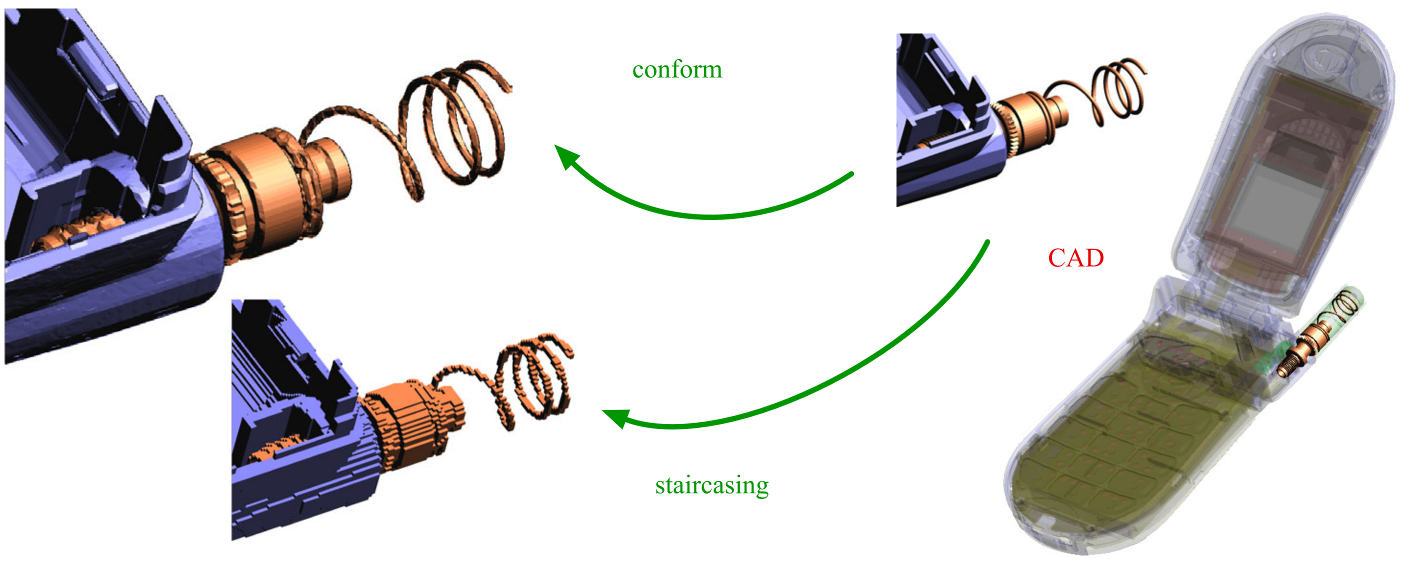

Figure 3: CAD representation, staircasing and conformal discretization of a commercial mobile phone with more than one hundert subparts, a grid of 166x426x186 and approximately 250000 surface triangles, conformally voxeled in 80 seconds on a P4, 2.8GHz.

Tolerances and Special Cases

The intersection calculation of a grid line with poorly shaped surface triangles can lead to significant numerical errors. The calculation is therefore performed with tolerances, e.g., with a tolerance strip around the triangle (see surface triangle in figure 5).

An additional benefit of the tolerance strip is to avoid distinguishing between different cases when the grid line is tangential to the surface triangle. In the literature (e.g., [4], virtual gridlines) it is distinguished between the cases depicted in figure 5. The tolerance strip enables easy but symmetric and robust discretization without differentiating special cases. The algorithm only investigates the entry/exit point pattern. If after an entry point an exit point follows, all is fine and the left case is automatically 'recognized'. If two entry points are next to each other, the right situation is automatically discretized and the algorithm does not use the second entry point, but the following point if it is an exit point.

Examples & Benchmarks

The capabilities of the conformal FDTD mesh generator have proven its general versatility in a wide range of real-world applications. In figure 2 a human model (head, hand) and mobile phone is shown, modeling the real-world situation of a phoning person. Figure 3 demonstrates the complexity of single parts of a commercial mobile phone model (antenna and case). Figure 1 shows a very detailed hearing aid model.

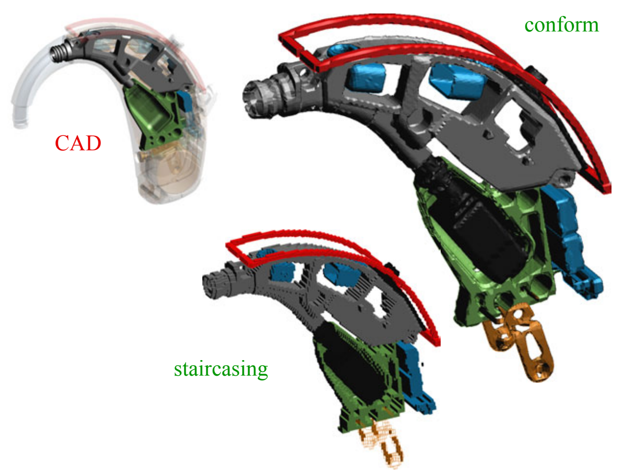

Figure 1: CAD representation, staircasing and conformal discretization of a commercial hearing aid with more than one hundert subparts, a grid of 49x130x145, approximately 200000 surface triangles, conformally voxeled in 12 seconds on a P4, 2.8GHz.

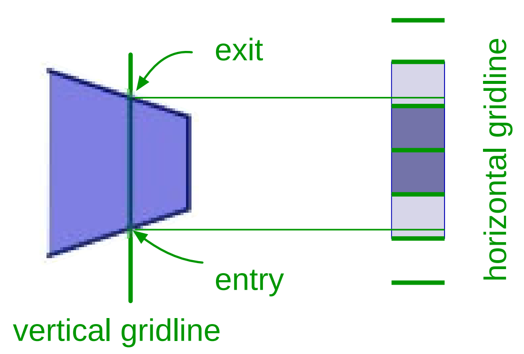

Figure 4: Scan conversion algorithm: the entry and exit points of an object hit by a grid line define the cells which are completely (dark blue) or partially (light blue) inside the object. Regardless of how many cells are between the entry and exit points, this kind of assignment scales according to the surface size instead of the object's volume size and thus the complexity is reduced. The technique can be used to assign a cell to its object, an edge to its object or a cut pattern of a conformal cell.

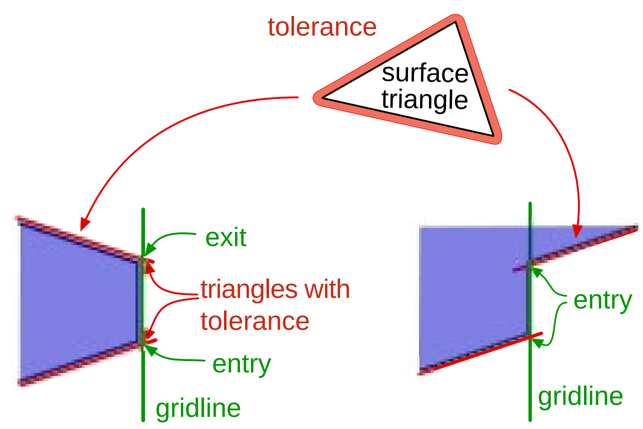

Figure 5: In the literature (e.g., [4]) it was reported that the two cases depicted in this figure needed to be handled differently . With a tolerance stip around the triangle (red) this problem is easily solved by looking at the entry/exit point pattern. If two entry points are in the list, then only the first one ist considered; if an exit point follows, all is fine. The technique is symmetrical and robust, and no special treatment is necessary. Furthermore the numerical inaccuracies are overcome without any additional effort.

Conformal FDTD Applications

IT'IS FOUNDATION
IIS ETH Zürich

METHOD: CONFORMAL FDTD

The conformal discretization described in the first section is the basis for conformal FDTD simulations. The additional geometric information is incorporated into the FDTD algorithm to reduce the material assignment based error while keeping the spatial and temporial resolution and its corresponding errors. In the literature (an overview in [2], state-of-the-art method in [3]) several attempts have been made to enhance accuracy.

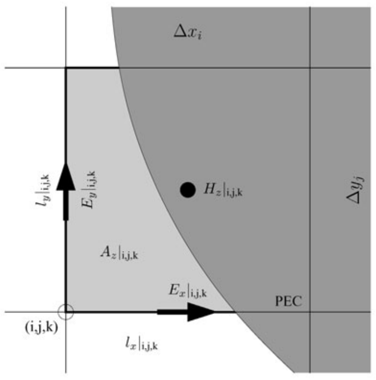

Figure 6: A loop for Faraday's law using the conventionally staggered grid. The lengths and area are the metal free parts.

The cited methods enhance the accuracy considerably; however some important details require improvement:

- modifications of the update stencil, e.g., split curl-coefficients (see equation (1))
- more multiplications per time step than conventional FDTD updating
- higher memory consumption than the conventional FDTD updating
- stability criteria: reduction of the time step without providing a proven formula (only guidelines based on experiments)

A new conformal FDTD method has been derived which overcomes these limitations. The details are not presented on this poster but will soon be submitted to AP.

Proposed Updating Scheme

In every conformal FDTD algorithm the magnetic field update is modified according to Faraday's law in the following way (see figure 6 for the common staggered FDTD grid notation):

$$H_z|_{i,j,k}^{n+1/2} = H_z|_{i,j,k}^{n-1/2} + \frac{\Delta t}{\mu \cdot A_z|_{i,j,k}} \cdot \Big(E_x|_{i,j+1,k}^{n} \cdot l_x|_{i,j+1,k} - E_x|_{i,j,k}^{n} \cdot l_x|_{i,j,k} - E_y|_{i+1,j,k}^{n} \cdot l_y|_{i+1,j,k} + E_y|_{i,j,k}^{n} \cdot l_y|_{i,j,k} \Big) \quad (1)$$

where E and H denote the electric and magnetic fields, Δt is the time step, n denotes the time step index, i, j, k are the spatial indices, μ denotes the permeability, and l and A are the PEC free length and area, respectively. This equation is used directly in the Dey-Mittra PEC model [3] (the conventional curl-coefficient ($\Delta t/\mu$) is split into four coefficients). The proposed method starts with the same equations but introduces some definitions to generate a more compact formulation. It combines ideas from the diagonal split cell [1] and the conformal approach in the above equation.

Stability

A great advantage of the proposed conformal FDTD algorithm is that a time step reduction can be mathematically derived and proven:

$$\Delta t_A^{\text{PEC model}} = \sqrt{\frac{A_A^{\text{ratio}}}{\max\limits_{\text{edge}\in A} \Delta_{\text{edge}}^{\text{ratio}}}} \cdot \Delta t_A \quad (2)$$

Written in a sentence: the conventionally calculated time step for the considered area (see figure 6) is reduced by the square root of the ratio of the PEC free area fraction and the maximal PEC free length ratio belonging to that area.

NUMERICAL RESULTS & BENCHMARKS

It is well known that conformal FDTD has proven its effectiveness for simulating resonating structures. To demonstrate its performance on near and scattered fields, Mie scattering was used to analytically compare the L_2 errors (volume integrated squared difference). The staircasing solution, the diagonal split cell model [1] and the proposed methods were investigated. The near and scattered E-field errors were compared to the analytical solution.

To increase the benchmark complexity and in order to demonstrate the versatility and robustness of the proposed update scheme, a real-world dual-band PCS/GPS antenna similar to the one in [5] was simulated (figure 11).

MIE SCATTERING

In the Mie benchmark simulations a plane wave excition is placed symmetrically around a sphere with a side length of approximately two thirds of the wavelength (3GHz was chosen). The spatial discretization varied from λ/12.5 to λ/100 whereas the radius varied from 5 (5/8 voxel) to 32mm (4 voxels) depending on the investigated effect. PML was used as the absorbing boundary condition. For all simulations the time step was chosen as 31% of the CFL time step according to equation (2).

Aligned Sphere

The performance of the algorithms was tested on spheres with radii of a multiple of the coarsest grid step (radius of one, two and three voxels). The solutions for four uniform grids were compared (λ/12.5, λ/25, λ/50, λ/100). In figure 7 the near field and in figure 8 the scattered field of the two-voxel-radius simulation are presented. For a discussion of the results see the captions.

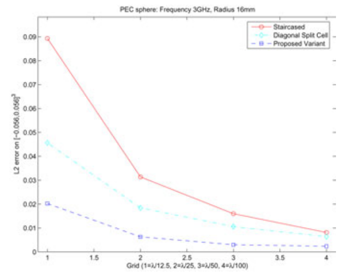

Figure 7: Comparison of the near field. With the proposed method one can save two refinements and with the diagonal split cell method one refinement. The advantage from gains in memory and simulation time to achieve the same accuracy is obvious, recalling that for a uniform grid the algorithm scales like N^4, where N is the number of elements along a single axis.

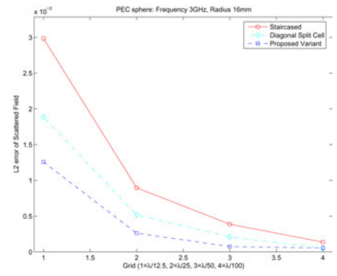

Figure 8: Comparison of the scattered field. On the coarsest grid the near to far field transormation introduces some integration errors. With the proposed method one can save two refinements and with the diagonal split cell method one refinement. The benefit in simulation time is again huge.

Non-Aligned Sphere

This benchmark compares spheres whose radii are not a multiple of a grid step. It is expected that the staircasing solution will depend heavily on the radius whereas the conformal model should be more constant. See the captions in figures 9 and 10 for a discussion of the results. The main conclusion: the smoothness of the error versus the radius in the conformal simulations is an excellent proof of the effectiveness of the proposed method.

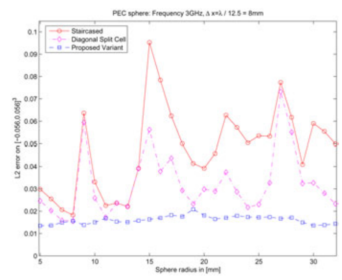

Figure 9: Comparison of the near field for different radii but the same grid resolution (λ/12.5). The proposed method is more accurate than the other schemes for every radius. The error of the proposed method varies only slightly with the radius, whereas the accuracy of the other two schemes strongly depends on the radius and the staircased representation.

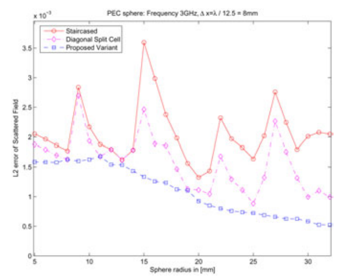

Figure 10: Comparison of the scattered field for different radii but the same grid resolution (λ/12.5). The proposed method is more accurate than the other schemes for every radius. The error of the proposed method varies only slightly with the radius whereas the accuracy of the other two schemes strongly depends on the radius and the staircased representation.

REFERENCES

[1] *Allen Taflove and Susan Hagness, Computational Electro-dynamics: The Finite-Difference Time-Domain Method, 2 ed., Artech House, Boston, MA, 2000.*
[2] *C. J. Railton and J. B. Schneider, An Analytical and Numerical Analysis of Several Locally Conformal FDTD Schemes, IEEE Transactions on Microwave Theory and Techniques, vol. 47, no. 1, 56-66, January, 1999.*
[3] *S. Dey and R. Mittra, A Modified Locally Conformal Finite-Difference Time-Domain Algorithm for Modeling Three-Dimensional Perfectly Conducting Objects, Microwave and Optical Technology Letters, vol. 17, no. 6, 349-352, April, 1998.*
[4] *T. Su, Y. Liu, W. Yu, and R. Mittra, A Conformal Mesh-Generating Technique for the Conformal Finite-Difference Time-Domain (CFDTD) Method,, IEEE Antennas and Propagation Magazine, vol. 46, no. 1, 37-49, February, 2004.*
[5] *J. Wu, J. Row, and K. Wong, A Compact Dual-Band Microstrip Patch Antenna Suitable For DCS/GPS Operations, Microwave and Optical Technology Letters, vol. 29, no. 6, 410-412, June, 2001.*

PCS/GPS DUAL-BAND ANTENNA

Within an additional benchmark, a dual-band antenna similar to the one in [5] was modeled and simulated. The antenna consists of a metal square ring (lower plate), which radiates in the GPS band and the upper square with two off-center metal rods which radiates in the PCS band. The PCS antenna is excited via a metal rod in the center of the square plate.

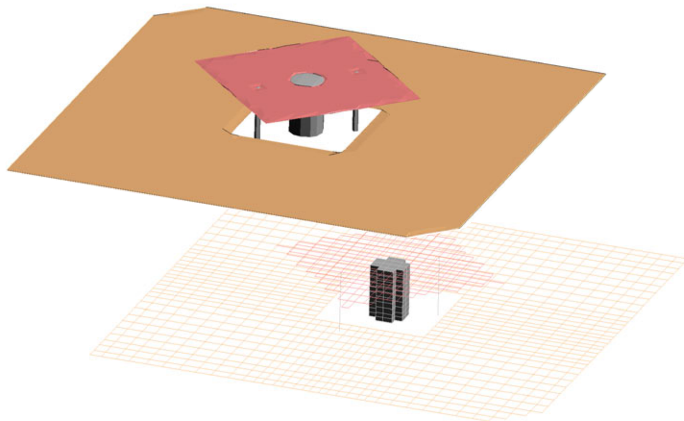

Figure 11: The conformal and staircasing discretization of the PCS/GPS dual-band antenna. All objects are PEC. The grid consists of 52x53x23 cells.

Because of the proven stability criteria, the conformal FDTD was always stable and the time step was chosen as 31% of the staircasing time step. PML was used as absorbing boundary condition and the grid resolution varies from 0.017 to 13.1 million cells (Mcells). The structure is excited at the center rod with a voltage source.

The return loss of the PCS antenna in figure 12 shows the excellent performance of the coarse conformal FDTD simulation compared to the staircasing ones with different resolutions. The gain in simulation time is tremendous as well as the savings of memory. Instead of 3 minutes simulation time in the conform run it took over 9 hours for the finest staircasing simulation and the computational cell requirements are almost 800 times larger.

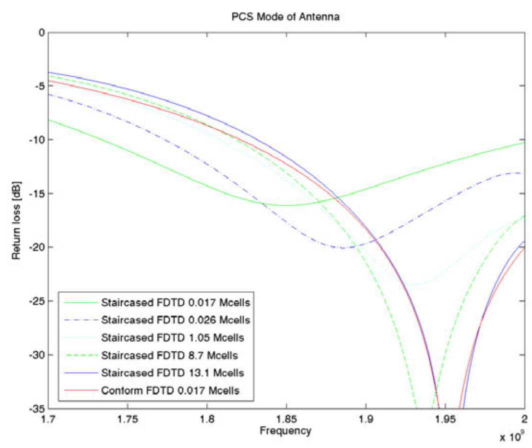

Figure 12: The conform FDTD on the coarsest grid simulation gives a return loss which can be achieved only on very fine staircasing simulations.

CONCLUSIONS

The major new contributions can be summarized as follows:

- New conformal FDTD updating scheme:
  - less memory consumption than current state-of-the-art model proposed in [3]
  - less multiplications per time step than model proposed in [3]
  - proven stability criteria
- Conformal Discretization:
  - introducing a tolerance strip around the surface triangle, the numerical difficulties of poorly shaped triangles are solved
  - in addition, there was no need to distinguish between special tangential cases
  - the speed was drastically enhanced using the scan conversion technique throughout the (conformal) discretization

The novel proposed and implemented conformal meshing algorithms and the locally conformal FDTD scheme enable improved spatial modeling and simulation of complex 3-D real-world structures. They were validated on the basis of benchmark examples as well as targeting complex industrial applications.

The new methods constitute a significant benefit and performance increase for electromagnetics related applications in general and for mobile communication and medicine in particular. With them, CAD datasets from industrial environments can be imported and reliably meshed within a few minutes. Moreover, the new 3-D conformal scheme demonstrated orders of magnitude in reduction of computational runtime and memory requirements, by maintaining the same order of accuracy.